NANOINDENTATION / NANOSCRATCHING AND STRESS STUDIES IN MONOLITHIC AND NANOLAYERED AMORPHOUS CARBON FILMS

S. LOGOTHETIDIS, C. CHARITIDIS AND M. GIOTI
Department of Physics, Aristotle University of Thessaloniki, 540 06 Thessaloniki, Greece.

Abstract

We have recently reported that monolithic amorphous carbon (a-C) films deposited by RF magnetron sputtering exhibit a high level of sp^3 sites when a negative bias voltage (V_b) is applied onto the substrate. This type of a-C films are dense (~2.65 g/cm^3), hard (>20 GPa) and highly stressed (6-7 GPa). The latter, however, limits their thickness below to ~40 nm. Thus, we have developed nanolayer structured a-C thick films with alternating V_b (positive / negative) which are stable, hard and rich in sp^3 content. Nanoindentation and low load scratch test results demonstrate that the layers rich in sp^2 content promote the stress relaxation of the films during a compositional rearrangement when a layer rich in sp^3 content is deposited. Possible explanations on the origin of the stress relaxation and the enhancement of the elastic properties in nanolayered a-C films are proposed and discussed based on the formation of compositional smooth interfaces between the two different types of layers.

1. Introduction

The use of sputter deposited amorphous carbon (a-C) thin films has enlarged in a wide range of technological and industrial applications, such as micro-electronic, optical, biomedical applications, wear-, corrosion-resistant materials and protective overcoats for hard disks in the magnetic storage industry. Sputtering offers a number of benefits such as low cost, process simplicity and control, and film homogeneity. It is also not time-consuming. All the above characteristics make sputtering an attractive and powerful technique for a-C production, especially for industrial scale production. The present trend in a-C thin film technology is largely dictated by the urgent need for the development of new processes, materials and their fabrication for applications in surface engineering and submicron microelectronics.

The high internal stresses as measured in sputtered a-C films are closely related to adhesion problems and crack creation in the films, and thus limit their maximum thickness for good adherence on the substrate at ~40 nm. Consequently, the search for processes reducing film stress, improving thermal stability and low toughness of a-C films, are some major technological challenges in a-C research. Recently, it has been

G.M. Chow et al. (eds.), Nanostructured Films and Coatings, 297–308.

shown that reduction of the internal stress in thick a-C films with high hardness can be obtained by developing layer structured (consisting of sequential soft and hard nanolayers) films [1].

Amorphous carbon films 30 nm thick, deposited with negative V_b were found to be rich in sp^3 sites (45%), dense (~2.65 g/cm^3) and with compressive stress above 6 GPa. On the other hand, films deposited with positive V_b are rich in sp^2 sites, exhibit low density (1.9 g/cm^3) and compressive stress (~1 GPa). It was also found that the development of a-C films in the form of nanolayered structure, consisting of sequential layers of the above mentioned two different types of a-C films, provides stable, thick and rich in sp^3 sites a-C films [1] potentially for many practical applications.

In this work, emphasis is placed upon the study of the elastic properties of these two types of a-C films and their dependence on the substrate bias voltage (Ar^+ ion energy). The enhancement of elastic properties and their comparison with those so far reported for sputtered a-C films, and the scratching behavior of nanolayered structures (consisting of sequential layers deposited with alternating V_b) are also presented. In view of the obtained results, possible explanations on the origin of the stress relaxation and enhancement of the elastic properties in nanolayered a-C films are proposed and discussed, based on the formation of compositional smooth interfaces between the different type of layers.

2. Experimental Details

The sputtered a-C films studied here were deposited in an Alcatel SCM 600 magnetron sputtering apparatus which has been described elsewhere [2,3]. Briefly, the a-C thin films were deposited on c-Si (001) substrates using a graphite (99.999% purity) target. During deposition, the sputtering Ar gas was at a partial pressure of 1.5×10^{-2} Torr, the target to substrate distance was fixed at 65 mm, and the discharge power equal to 100 W. The only parameter that was varied was the substrate bias voltage V_b. A phase modulated ellipsometer, mounted on the deposition system, allows in-situ and real-time spectroscopic ellipsometry (SE) measurements in the energy region 1.5-5.5 eV, and was used to estimate the thickness and the composition (sp^2 and sp^3 content) of the deposited film [3].

To investigate the mechanical behavior of a-C thin films three series of a-C films with thickness 30, 280 and 200 nm, respectively, were prepared. The a-C films with thickness 30 nm were deposited either with negative or positive V_b and those of 200 nm thick with positive V_b. The films with thickness 280 nm were deposited in sequential thin layers with alternating (positive/negative) V_b. In detail, first a layer of ~15 nm was deposited with V_b=+10 V and consequently a layer of ~23 nm with V_b=-20 V. In the next bilayers the thickness of each one was ~5 nm and ~23 nm, respectively, for the development of films with total thickness ~280 nm. We have found by analyzing SE (nanoindentation) measurements that films deposited with negative V_b were rich in sp^3 content (hard), while films deposited with positive V_b were rich in sp^2 content (soft) [4].

The elastic (hardness, H and elastic modulus, E) and tribological properties of the films were conducted using a Nano Indenter XP system with the continuous stiffness measurements (CSM) and lateral-force measurements (LFM) options. The H and E of

each of the films were measured with a Berkovich, three-sided pyramid diamond indenter with nominal angle of 65.3° between the tip axis and the faces of the triangular pyramid, which was forced into the specimen surface by using a coil and magnet assembly. Nanoindentation measurements were obtained with both conventional indentation (CI) and CSM. The system has load (displacement) resolution of 50 nN (<0.01 nm). A detailed description of the system has been presented elsewhere [5]. Prior to each indentation test, two indents in 100 nm depth were conducted in fused silica to evaluate the tip condition. When CSM technique [5,6,7] is employed, the stiffness is measured continuously allowing the H and E to be calculated at every displacement point acquired during the indentation experiment. In all CI and CSM depth-sensing tests a total of ten indents were averaged to determine the mean H and E values for statistical purposes, with a spacing of 50 μm.

A different diamond Berkovich indenter was used for scratch testing. Scratches were made with an edge of the indenter (point-on orientation). Prior to each scratch test, three indents were made in aluminum to clean the tip, and then two 100 nm indents were made in fused silica to evaluate the condition of the tip. A precision X-Y table with a resolution of 1 μm was used to slide the film under the tip with a minimum of vibration and electrical noise. Lateral deflection was measured using two separate capacitive displacement gauges to sense the lateral displacement of the indenter column in the X and Y directions. Lateral (friction) forces were then calculated from stiffness of the column determined in calibration experiments. Coefficient of friction (μ) can be calculated afterwards [8]. Since scratch-induced damage of a film, specifically fracture or delamination, was monitored by in-situ friction force measurements there was no need to obtain an image of the scratch event but only to confirm the experimental results. Depths of scratches with increasing scratch length or normal load were measured in-situ by profiling the surface of the film before, during and after the scratch event, resulting in a total length of the test of 700 μm, while the scratch length was 500 μm long. The load for initial and post-scratch scan was 0.02 mN. Data from these regions were used to account for both the slope and curvature of the sample surface so that the entire scratch can be viewed with the surface of the sample as the baseline for deformation [9].

Stress measurements were immediately performed after each layer or thin film was deposited and exposed to air. The stresses were measured using a commercial instrument by Tencor, and calculated by measuring the radius of the curvature of the substrate before and after film deposition by the modified Stoney expression [3]. The films were also studied by Transmission Electron Microscopy in cross-section geometry (XTEM) [10].

3. Results and Discussion

3.1. MECHANICAL PROPERTIES OF a-C FILMS, AND THEIR DEPENDENCE ON V_b AND THICKNESS

Figure 1 shows the plots of hardness and elastic modulus as a function of contact depth obtained from two a-C films, deposited with V_b=+10 and -10 V, with the same

thickness 30 nm. For the film deposited with V_b=-10 V the maximum H (E) value was ~18 (185) GPa, whereas that deposited with V_b=+10 V was ~8 (130) GPa. Since the a-C films were deposited on Si, their hardness (elastic modulus) approaches at large contact depths, the value of Si, 12.5 (168) GPa. The above values of H and E for each V_b were estimated from the regime of the shallow data points (Fig.1) as more representative of the film properties. Hardness of hydrogenated carbon films with almost the same thickness was found to be 9.4 GPa [11].

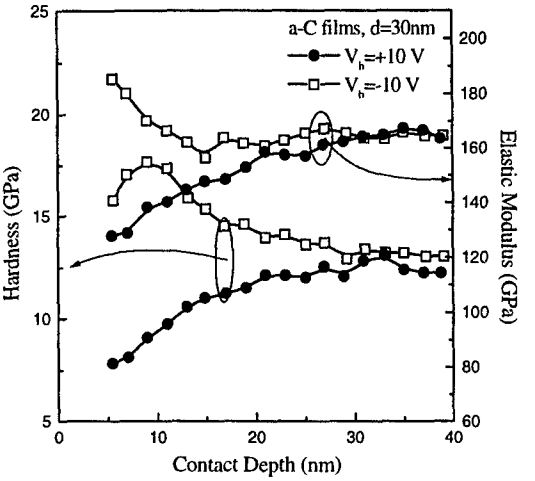

Figure 1. Nanoindentation data of H and E vs. indentation contact depth obtained from single a-C films 30 nm thick, deposited with V_b=+10 V (circles) and V_b=-10 V (squares). The CSM data obtained in contact depth 40 nm.

The development of a-C films rich in sp^3 C-C sites is based on incident energetic species (neutrals or ions) that penetrate the growing surface and induce subsurface growth [12]. A negative V_b achieves the energetic ion bombardment during sputter deposition [3,13,14]. Films produced with positive V_b exhibit low hardness because the mean energy of the deposited neutral species is lower than a critical one to penetrate the film's surface. Thus, in these films the sp^2 bonding is dominant, both hardness and density [15] are low and the films exhibit a large amount of voids [16]. We measured in these films a sp^2 (sp^3) volume fraction ~60 (20)% and density 1.9 g/cm^3. When a negative V_b is applied the Ar^+ ions are oriented towards the substrate with kinetic energy E, which in first approximation is given by the following expression: $E=e|V_b|+E_o$, where E_o is the mean energy of the discharge. The transfer of energy from Ar^+ ions to deposited C species results in the formation of rich in sp^3 C-C bond films [15,16]. The results from SE data analysis [5] have shown that when V_b=-10 V promotes the formation of sp^3 sites (~50%) all over the film (except the initial stages of growth) resulting in a hard material with density, measured with X-ray reflectivity, 2.6 g/cm^3 [15]. The above experimental data and the qualitative interpretation suggest that an interrelation exist between the hardness and elastic modulus and the sp^3 bonding of a-C films.

The dependence of hardness on the V_b for a-C films, 30 nm thick, is shown in Fig. 2. The elastic modulus exhibits the same dependence on V_b with the hardness. Both of these quantities do not exhibit the same dependence with the sp^3 content [17] on V_b. There is a sharp increase in going from positive (the film is rich in sp^2 content) to negative V_b (rich in sp^3 content). In the regime -100 V<V_b<0 V (30-130 eV, low energy ion bombardment) there is a near plateau in H and E values that indicates the existence of a subplantation mechanism (probably indirect) during deposition. That is, Ar^+ transfer their energy to the surface C atoms which subplant below the surface. In the energy window 30-130 eV the produced a-C films were rich in sp^3 sites and hard. For V_b<-100 V (ion energy above 130 eV) it was found a reduction in stress (Fig. 3a), which in concurrent with the decrease of the sp^3 content but not with density [17].

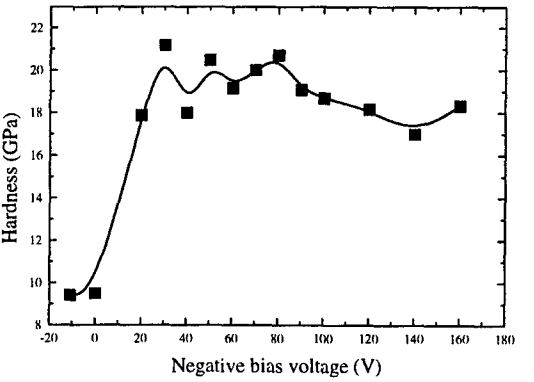

Figure 2. Hardness of sputtered 30 nm thick a-C films versus Vb. The data was obtained from indentations at a contact depth of 20 nm using the CSM technique.

The dependence of compressive stress on the V_b for a-C single films, 30 nm thick, is shown in Fig. 3a. Stress exhibits the same dependence with the sp^3 content on V_b, as proposed by the densification model [18,19]. There is a sharp increase in going from ground to negative V_b and a broad non-symmetric peak at V_b=-40V. The stress behavior can be described successfully by Davis' formula [19]. Stress values measured at films deposited with negative (positive) bias voltage support that stresses in a-C films are an intrinsic property and arise from the deposition mechanism that creates the sp^3 (sp^2) bonding. The film deposited in sequential layers with alternating V_b leads to the development of stable and highly sp^3 bonded material. Figure 3b shows the evolution of stress with the thickness for the nanolayered structure film 280 nm thick. The first deposited soft layer exhibits low stress (1.35 GPa). Consequently, it provides good adhesion of the film to the substrate. The next deposited hard layer increases rapidly the average stress of the film to 4.5 GPa. Further depositions of layers either with positive or negative V_b do not affect much the situation that was established during the deposition of the first two layers. Above the 180 nm film thickness the stress values saturate to ~5.2 GPa.

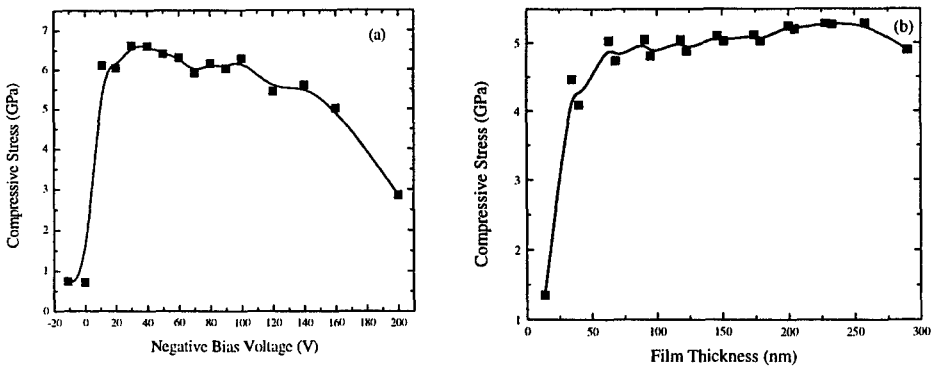

Figure 3. The variation of compressive stress of single a-C films vs V_b (a), the evolution of stress with thickness in an a-C film in sequential layers with alternating V_b (b).

What is important about the nanolayer a-C film is that there are large stress gradients in the film between the individual layers. Even the average stress is relative small (~5.2 GPa, Fig. 3b) within the sp^3 layers, stresses are larger. The resulting large stress gradients in the film can act as an additional driving force for atomic diffusion at the sp^3-rich to sp^2-rich interfaces.

3.2. ENHANCEMENT OF ELASTIC PROPERTIES AND STRESS RELAXATION IN NANOLAYERED a-C FILMS

Figure 4 shows the nanoindentation results for an a-C film 280 nm thick, where H and E are plotted as a function of contact depth.

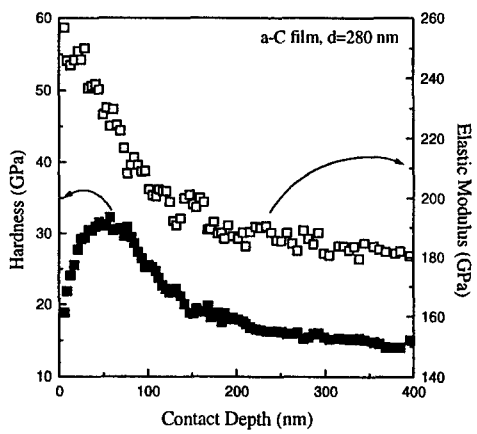

Figure 4. Hardness and elastic modulus vs. indentation contact depth obtained from a-C films 280 nm thick, deposited in sequential layers with alternating V_b using the CSM technique.

Indentation was conducted by applying both the CI, in different contact depths, and the CSM technique for penetration depth 400 nm. At shallow depths, about 20-50 nm,

elastic properties more representative of the films were obtained but still influenced by the substrate. Comparing these values of H and E with those obtained from an a-C:H film (H=17 and E=175 GPa), 300 nm thick prepared by sputter deposition on Si [20], we conclude that hydrogen-free a-C film deposited in sequential layers with alternate positive/negative V_b of layers are harder by a factor of ~2.

Figure 5 compares the load-displacement curves for 30 nm thick a-C films deposited either with positive or with negative V_b, both tested with identical indentation cycles to a maximum load of 0.11 mN. Low-load indentation experiments have revealed that a-C films deposited with positive V_b exhibit more plastic deformation than those developed with negative V_b. Figure 6 shows representative CI load-displacement curves for 200 and 280 nm thick a-C films at specific loads to achieve contact depths at the same percentage (~12%) of each one thickness.

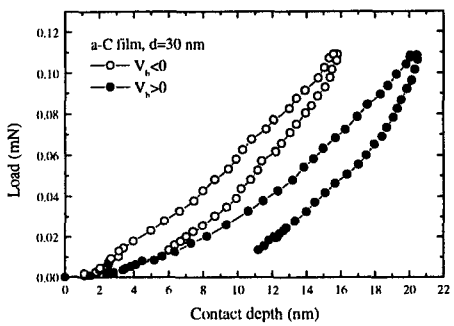

Figure 5. Load-displacement curves for 30 nm thick a-C films deposited with positive and negative V_b at the same maximum load.

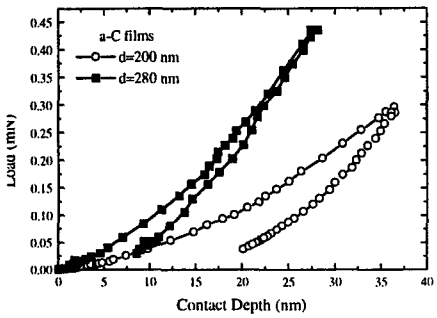

Figure 6. Load-displacement curves for 200 and 280 nm thick a-C films obtained at a penetration depth of about 12% of film thickness.

Figures 5 and 6 display the qualitative differences between the three series of a-C films concerning not only their hardness but their elastic deformation behavior, too. From the maximum penetration depth and the residual depth for each case, we have found that a-C films deposited in sequential layers by altering V_b exhibit much higher hardness and elastic deformation ~80% than the films deposited with V_b>0, ~50% and higher to those deposited with V_b<0, ~70%.

The film deposited in sequential layers with alternating V_b leaded to the development of stable and rich in sp^3 bonded material, resulting in harder a-C films than the ones developed solely with negative V_b (Fig. 1). The deposited layers with V_b>0 seem to be essential for the stress relaxation of the whole film and was made practicable to grow thicker and stable a-C films [1].

In order to study the geometrical characteristics of the nanolayered structure of the a-C films we performed an XTEM study of the a-C specimens [10]. As it is shown in Fig. 7, the film consisted of 10 bilayers with almost the same modulation period ~26 nm, except the first one on the top of the substrate (~35 nm) and an ultra-thin layer (~1.5 nm), which was deposited with V_b=+10 V, on top of the film. Since the layers had the same chemical nature (amorphous carbon), the existing contrast difference indicates the different bonding and density in the layers. Thus, the light colored layers are attributed to the sp^2-rich layers whereas, the dark colored to the sp^3-rich ones. From the

XTEM [10] and SE and XRR [21] results, modifications in thickness and composition of soft layers were found to occur during the deposition of hard (rich in sp^3 bonds) layers. Namely, a reduction in the thickness of soft layers was observed when a hard layer was deposited on it.

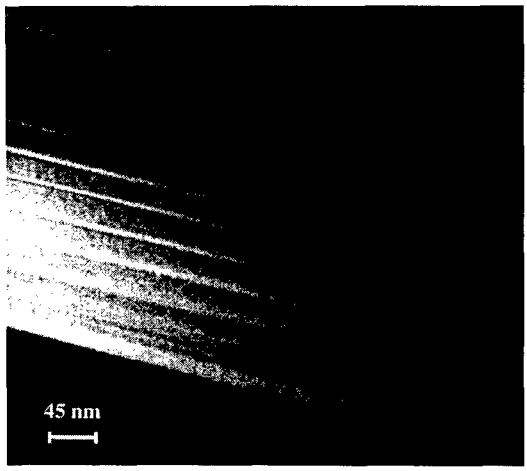

Figure 7. A TEM cross-section image of nanolayer a-C film made of alternating rich in sp^2 / rich in sp^3 layers.

3.3. NANOSCRATCH TESTS ON NANOLAYERED a-C FILMS

The objective of the nanoscratch tests was to investigate the elastic and tribological properties of the films developed in layered structure (rich in sp^3 content) and their comparison with those of films rich in sp^2 content. We focused on the adhesion and deformation response of the films using the scratch test as main experimental characterization tool. Film deformation response was studied in order to gain a better understanding on the mechanisms governing the failure of thin films.

In Fig. 8 nanoscratch test results for a-C films, 280 nm thick, at various normal loads are presented. Figure 8 includes plot of the vertical displacements of the diamond during the initial scan (prescan), the load-ramped scratch (scratch scan), and the post scratch scan (post scan) for each film. The scratch proceeds from left to right in the figure. The initial scan profiles the unscratched surface of the film and the post-scratch scan was used to determine the surface damage due to the scratch event. Negative displacements correspond to the scratch tip being pushed into the specimen, and positive displacements that appear in the post-scratch scan, indicate the outward blistering of the surface or the accumulation of debris in the scratch trace. Four scratches were made at each load at different areas of specimen.

In Fig. 8a the scratch can be divided into two regimes based on differences in the appearance of the scratch profile. The first regime was defined by the first 300 μm of the scratch. In this regime, the scratch is extremely smooth and shallow as can be seen both by comparing the post scan to the prescan and by optical microscopy. A closer examination revealed that there are no remnants of the scratch, corresponding to fully recovered elastic contact. The second regime extended from 400 to 600 μm. In this

regime, film recovery was highly elastic (~90%). It is marked by a change in the scratch displacement. In this regime, the film blisters by partial delamination between layers [9]. Examination of the film by optical microscopy revealed an amount of small particle debris surrounding the scratch trace in this regime, suggesting that damage was limited to cracking and small areas of pull-off contained entirely within the scratch track.

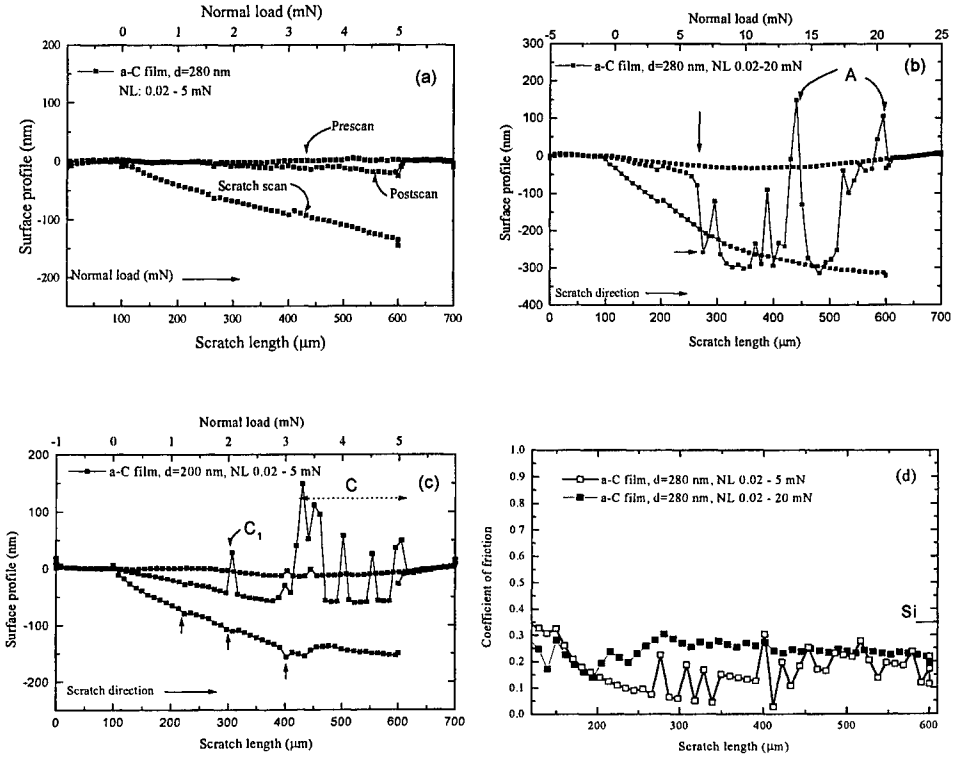

Figure 8. Surface profiles of the a-C films rich in sp^3 content developed in nanolayered structure, 280nm thick, scratched with ramping normal loads of 0.02 – 5 mN (a) and 0.02 – 20 mN (b), and a-C films rich in sp^2 content (200 nm thick) scratched with ramping normal loads of 0.02 – 5 mN (c). Coefficient of friction profiles of a-C films rich in sp^3 content, 280 nm thick, as a function of scratching length (ramping normal load) (d).

The behavior of the a-C film, 280 nm thick at load up to 20 mN, was examined to monitor the adhesion and strength of the film. As shown in Fig. 8b, the regime from 100 to 250 μm was characterized by almost fully elastic recovery. In the regime above 250 μm (i.e. load above 5 mN) there was a large change in post scan, failure begun abruptly by brittle fragmentation in the film and substrate. The post scan trace showed that the fragmentation has occurred at a depth near the film thickness, indicating complete failure and removal of the film [22,23] (position A in Fig. 8b). In details, the height measured at position A is ~150 nm, and it was the half of the film thickness, which also implies the absence of a significant portion of the a-C film, at a load ~14 mN.

Deformation response of the a-C film rich in sp^2 content (Fig. 8c) was mainly plastic all over the scratch length, and at ~400 μm of the scratch length (i.e. load 3 mN) failure begun abruptly by brittle fragmentation in the film. The ripple structures (observed in area C in Fig. 8c) pronounced along the track seems to be influenced by the tensile-type cracks. The depth measured in area C is ~150 nm, and it was more than the half of the film thickness, which implies the absence of a-C film at a load >3 mN and possibly is correlated to the delamination of the film. The poor adhesion of the a-C film to the substrate produced cracks and small regions of film pull-off at loads above 1mN, which resulted in the displacement roughness at scratch track positions between 200 and 300 μm (indicated by arrows in Fig. 8c). The large positive displacements between 300 and 600 μm represent the positions at which the stylus was forced over the delaminated film that was piled up in its path. Friction coefficient values for these films were found to be ~0.35.

Figure 8d is a plot of the friction coefficient (μ) versus scratch length (normal load) for a-C film 280 nm thick. The μ was calculated by taking the ratio of the lateral force and normal load on the indenter [8]. Until the tip begins to slide with respect to the sample, the μ is indeterminate. At the start of the scratch, the lateral force data is noisy indicating a stick-slip phenomenon [24]. Once the normal load reaches about 0.5mN, the μ settle to nearly constant values. Friction coefficient values for these films were found to be ~0.2, below those for a-C films rich in sp^2 content. Figures 8a,b and 8d show that both scratch depth and μ, respectively, increase with increasing scratch load. Friction coefficient clearly increased at, or close to, the point at which the film blisters (at ~300 μm of the scratch length, Fig. 8a) or detaches begun (at ~250 μm, Fig 8b). The measured increase in μ could be due to the indenter climbing over small (large) particle debris, for a scratch load 5 (20) mN, as it passes over the surface. The fluctuation in friction coefficient values is promoted by point-on orientation of the tip or the layered structure of the films or it could be due to nanoscale fracture events.

Based on the above findings we will discuss the possible explanations of the stability and the enhancement of the elastic properties of the nanolayered structured, rich in sp^2/sp^3 content a-C films. The soft (plastic) layers, deposited with $V_b>0$, seem to act as a reservoir of energy transferred to the film. As a result the soft layer sandwiched by the two elastic hard layers may not easily deform even under loading. An explanation for this behavior can be the following. The layered structure of the film with a smooth compositional transition at an interface (the layers have the same chemical nature but different bonding and density), is thought to result in preventing penetration of cracks into the film across an interface due to the difference in mechanical properties of two alternating layers. A compositional smooth interface can prevent the delamination of layered structured films at an interface providing the noticeable stability and adhesion of the layered structured films. The lamination of plastic and elastic layers prevents the energy from dispersing into the deeper layers or the substrate by causing an elastic displacement in the hard layer.

The material removal, with the formation of surface materials on the side of the scratch which were plastically torn away, indicates that scratching on films rich in sp^2 content took place mainly by plastic deformation typical of soft materials. This type of deformation of soft layers is possibly responsible for delamination and buckling effects observed in nanolayered structure films when the former are subjected to high normal

loads during the scratch test. A detailed examination of the scratch profiles in nanolayered structure films supports the above speculation. For the design of tough nanolayered structure a-C films we have to take into account the following mechanisms: i) the stress relaxation in the hard layer by plastic deformation in the soft layer [1], and ii) the termination of cross-sectional cracks by their deflection at interfaces and braking in a soft layer with energy dissipation by plastic deformation. For a-C nanolayered structure films the important question is whether the termination of plastic deformation in a soft layer is required. From the strengthening mechanisms, (i) and (ii), interlayer plasticity is necessary to blunt cracks and relax stresses in hard a-C bilayers. Thus, a minimum thickness of the soft layer is required to activate strengthening mechanisms (i) and (ii) for a-C layered structure. However, for larger soft layer thicknesses, there is a probability of failure of the total film stack by buckling or crack propagation along the soft layer. In conclusion, an optimal thickness of the individual layers is thought to be critical in the design of layered structure films with good properties. On the other hand, a layered structure film with a high number of interfaces exhibits an increase in toughness and crack propagation resistance [25]. Interfaces in films with layered structure are sites of energy dissipation and crack deflection leading to a toughening of the layer material. Further studies are in progress to determine the minimum thickness of soft layers and the number of interfaces in order to produce films with improved adhesion and toughness under high local loading and to reduce the amount of residual compressive stresses associated with the kinetically forced formation of sp^3 bonds in hard layers.

4. Conclusions

Hardness and elastic deformation enhancement for nanolayered structured films has been thought to occur possibly because of the formation of a compositional smooth interface when a rich in sp^3 sites layer deposited on a rich in sp^2 sites layer. Further work, however, is required to completely unravel the complex phenomena related to structure, processing and properties in this interesting and promising class of a-C films. This will allow us to understand the mechanisms of the elastic properties enhancement.

The results of the systematic investigation of scratch performance of sputtered a-C films in this work confirm the enhanced elastic behavior of the nanolayered films. Nanolayered films exhibit better adhesion strength comparing with those that are rich in sp^2 content, so that they can sustain film cracking without debonding. The direct and in-situ depth measurement can provide the elastic/plastic depth profile along the scratch track. Application of this useful information in scratch process, modeling and understanding of fundamental mechanisms may lead to increased toughness and adhesion of hard a-C films.

5. Acknowledgements

This work was supported in part by the Greek General Secretariat of Research and Technology.

6. References

1. Gioti, M., Logothetidis, S. and Charitidis, C. (1998) Appl. Phys. Lett. **73,** 184.
2. Logothetidis, S. (1996) Appl. Phys. Lett. **69,** 158.
3. Logothetidis, S. and Gioti, M. (1997) Mater. Sci. Eng. **B 46,** 119.
4. Charitidis, C., Logothetidis, S. and Douka, P. (1999) Diam. Relat. Mater. **8,** 558.
5. Logothetidis, S. and Charitidis, C. (1999) Thin Solid Films (in press).
6. Oliver, W.C. and Pharr, G.M. (1992) J. Mater. Res. **7,** 1564.
7. Nano Instruments, Inc. (1997) Nano Indenter® XP, Operating Instructions V1.1.
8. Scharf, T.W. and Barnard, J.A. (1997) Thin Solid Films **308-309,** 340.
9. McAdams, S.D., Tsui, T.Y., Oliver W.C. and Pharr, G.M. (1995) MRS Symp. Proc., **356,** 809.
10. Logothetidis, S., Gioti, M., Charitidis, C., Patsalas, P., Arvanitidis, J., Stoimenos, J. (1999) Appl. Surf. Sci. **138-139,** 244.
11. Wei, B. and Komvopoulos, K. (1996) ASME Journal of Tribology **118,** 431.
12. Lifshitz, Y., Lempert, G.D. and Grossman, E. (1994) Phys. Rev. Lett. **72,** 2753.
13. Ullmann, J., Schulze, S., Erben, J, Grunewald, W., Heger, D., Muhling, I. (1992) Thin Solid Films **219,** 109.
14. Schwan, J., Ulrich, S., Theel, T., Roth, H., Ehrherdt, H, Becker, P. and Silva, S.R.P. (1997) J. Appl. Phys. **82,** 6024.
15. Logothetidis, S. and Stergioudis, G. (1997) Appl. Phys. Lett. **71,** 2463.
16. Gioti, M. and Logothetidis, S. (1998) Diam. Relat. Mater. **7,** 444.
17. Logothetidis, S., Gioti, M., Patsalas, P. and Charitidis, C. (1999) Carbon **37,** 765.
18. Robertson, J. (1994) Diam. Relat. Mater. **3,** 361.
19. Davis, C.A. (1993) Thin Solid Films **30,** 226.
20. Tsui, T.Y, Pharr, G.M., Oliver, W.C., Bhatia, C.S., White, R.L., Andres, S., Anders, A. and Brown, I.G. (1995) Mat. Res. Soc. Symp. Proc. **383,** 447.
21. Logothetidis, S., Gioti, M., Charitidis, C., Patsalas, P. (1999) Vacuum **53,** 61.
22. Deng, H., Scharf, T.W. and Barnard, J.A. (1997) J. Appl. Phys. **81,** 5396.
23. Li, X., Bhushan, B. (1999) Thin Solid Films **340,** 210.
24. Li, K., Ni, B.Y., Li, J.C.M. (1996) J. Mater. Res. **11,** 6.
25. Holleck, H., Schier, V. (1995) Surf. Coat. Technol. **76-77,** 328.